DETECTION AND SIZING OF FATIGUE CRACKS IN STEEL WELDS WITH ADVANCED EDDY CURRENT TECHNIQUES

E. I. Todorov, W. C. Mohr, and M. G. Lozev

EWI, Engineering and NDE, 1250 Arthur E. Adams Dr., Columbus, OH 43221-3585

ABSTRACT. Butt-welded specimens were fatigued to produce cracks in the weld heat-affected zone. Advanced eddy current (AEC) techniques were used to detect and size the cracks through a coating. AEC results were compared with magnetic particle and phased-array ultrasonic techniques. Validation through destructive crack measurements was also conducted. Factors such as geometry, surface treatment, and crack tightness interfered with depth sizing. AEC inspection techniques have the potential of providing more accurate and complete sizing flaw data for manufacturing and in-service inspections.

Keywords: Eddy current testing, Advanced eddy current techniques, Weld inspection, Fatigue crack detection, Weld crack sizing.
PACS: 81.70.Ex, 81.20.Vj

INTRODUCTION

The U.S. has a highly developed transportation network. Much of the job of carrying the loads falls to steel structures (bridges, cranes, forklifts, conveyors, etc.) butt and fillet welded together and covered with a corrosion-prevention coating such as galvanizing or paint. During the service lifetime, some damage will be obvious, but other damage types, such as fatigue cracking, may be hidden under the coating until near the end of the useful lifetime. If the fatigue damage is not detected or monitored, catastrophic failure of the structure may occur causing severe financial loss or even loss of human life.

Several methods are currently employed for nondestructive evaluation (NDE) of steel structures and joints in service. Liquid-penetrant inspection requires complete removal of the protective coating and paint. Magnetic particle (MP) inspection is the method mostly used for steel-welded structures and joints. The MP techniques will also require removal of the coating. For many surface structures, radiography is not possible to perform due to accessibility requirements. All three techniques provide the length of the flaw only. More often, the flaw depth is the parameter determining structure safe life and repair actions. Ultrasonic (UT) conventional and advanced [phased-array (PA)] techniques are used extensively for length and depth sizing. However, the UT performance for small surface crack detection and sizing may not be adequate, particularly through coatings. Coatings may have to be removed to conduct reliable UT.

Two major advantages make the eddy current method particularly attractive for this type of structure and joint:

- No coating removal is required for inspection purposes.
- In addition to flaw length data, the eddy current equipment could possibly provide flaw depth data if adequately optimized and calibrated.

Eddy current array and single sensors provide new opportunities for inspection of these structures. Through advanced signal processing, eddy current probes produce superior data presentation, thus, significantly improving flaw detectability and inspection productivity. Significant cost benefits will be realized due to reduction of inspection time, improved detection capabilities, and faster data interpretation.

The project work focused on verifying the eddy current technique performance and approach for detection and sizing of flaws in welded structures and joints when common calibration procedures are used. In addition, this study addressed the effect that steel surface treatment (shot peening, grinding, machining, roughness, and others) had on the inspection process.

PREPARATION OF EXPERIMENTAL SPECIMENS AND BASELINE INSPECTIONS

The fatigue test specimens were fabricated from ASTM A572 Grade 50 steel plate, 12.7-mm (0.5-in.) thick. The plate was cut into pairs of plates, each 457 × 914 mm (18 × 36 in.) that were beveled with matching bevels to be re-joined across a 914 mm (36 in.)-long butt weld. Four of these butt-welded plates were made, using E71T-1 flux-core welding electrode. The butt weld was made with six passes, the first from the root side followed by gouging to smooth bare metal and grinding the cap of that pass smooth. MP testing was performed on the butt weld after welding.

The butt-welded plates were cut into 200-mm (8-in.)-wide strips across the butt weld. A batch of 16 specimens was prepared for shot peening. The entire specimen was peened, except for a masked region centered on one cap-side weld toe. This masked region was 25-mm (1-in.) wide and 100-mm (4-in.) long along the weld toe in the center of the weld length on the specimen. Only one of the two cap-side weld toes was masked. The masking tape was removed before fatigue testing as shown in Fig. 1.

In addition to MP of welds, conventional and advanced eddy current (AEC) inspection was performed on the weld crown and on 76-mm (3-in.) strips of metal surface on each side of the weld on top and bottom surfaces. The weld crown and heat-affected zone (HAZ) required several scans to cover the entire surface. Cracks or other flaws that might affect fatigue test were not detected during the inspection with conventional eddy

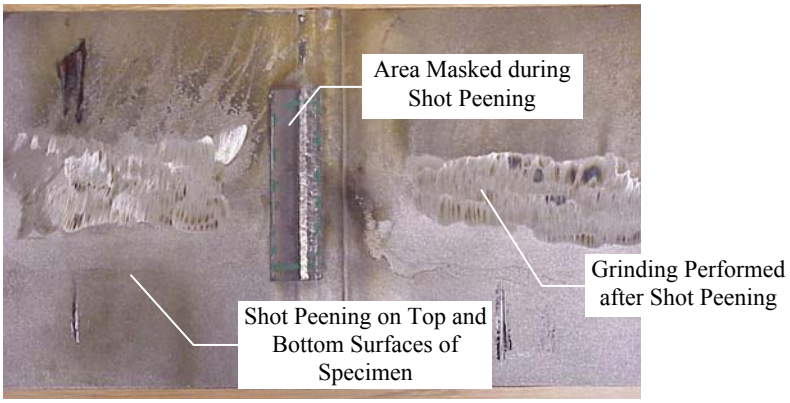

FIGURE 1. Specimen with butt weld and three surface areas – shot peened, masked, and ground. The entire bottom surface was shot peened.

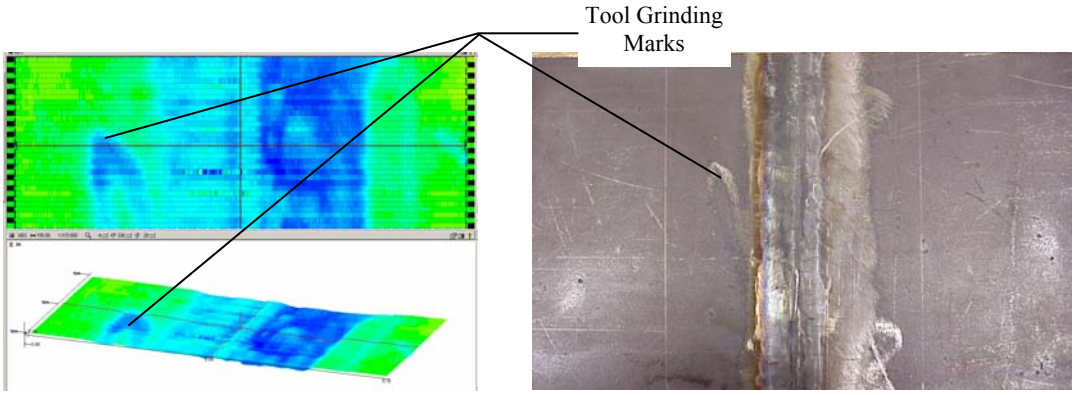

FIGURE 2. Typical grinding mark indications on specimen bottom surface.

current techniques. Thirteen scans with an array eddy current probe were conducted on the top and bottom surface around the weld. Cracks were not detected during the array probe inspection.

Other types of indications seen on all top and bottom surface scans were score and grinding marks (Fig. 2). Grinding of metal surface changes electrical conductivity and magnetic permeability of material, thus, creating indications shown in Fig. 2. The indications in Fig. 2 indicate the high sensitivity of eddy current method to any surface conditions and discontinuities.

Initially, the specimens were loaded in tension and welded attachments (later removed, hence the two ground areas) were used to localize the cracks at the masked area (Fig. 1). The fatigue crack initiation, though, was difficult to control. Later, the fatigue loading cycles were applied in three-point bending to the specimens and fatigue cracks were initiated and grown in the masked area at the butt weld toe. The span length between the outer rollers was 254 mm (10 in.). The central roller was placed at the ground root of the butt weld. Fatigue loading was performed under load control with displacement limits set to allow formation of fatigue cracks along the weld toe but to avoid large cracks or complete fracture. The stress range was chosen to limit the number of separate initiations of fatigue cracks along the weld toe. Fatigue cracks were grown in seven specimens, designated W12, W13, W14, W24, W33, W41, and W44. The first digit indicated the number of the long butt weld, while the second digit indicated the position along that weld. So W12, W13, and W14 were adjacent sections of the same weld.

MODELING OF EFFCTS OF VARIOUS PARAMETERS ON FLAW DETECTION AND SIZING

Typically, physical specimens and full-scale mockups with embedded natural and artificial flaws are used for optimization and later for validation. The experiments with specimens are complex, expensive, and time consuming when a large number of parameters influence the NDT technique performance. Currently, computer simulation and modeling are tools that help bridge the gaps in traditional approaches and minimize significantly the developmental costs.

The eddy current inspections were modeled with three-dimensional (3D) finite-element modeling (FEM) software. It is necessary to know steel electromagnetic properties - electrical conductivity (σ) and magnetic permeability (μ) to make model predictions more representative. The approach involved model optimization of probe interaction with inspected material to match field measurements for the same probe and

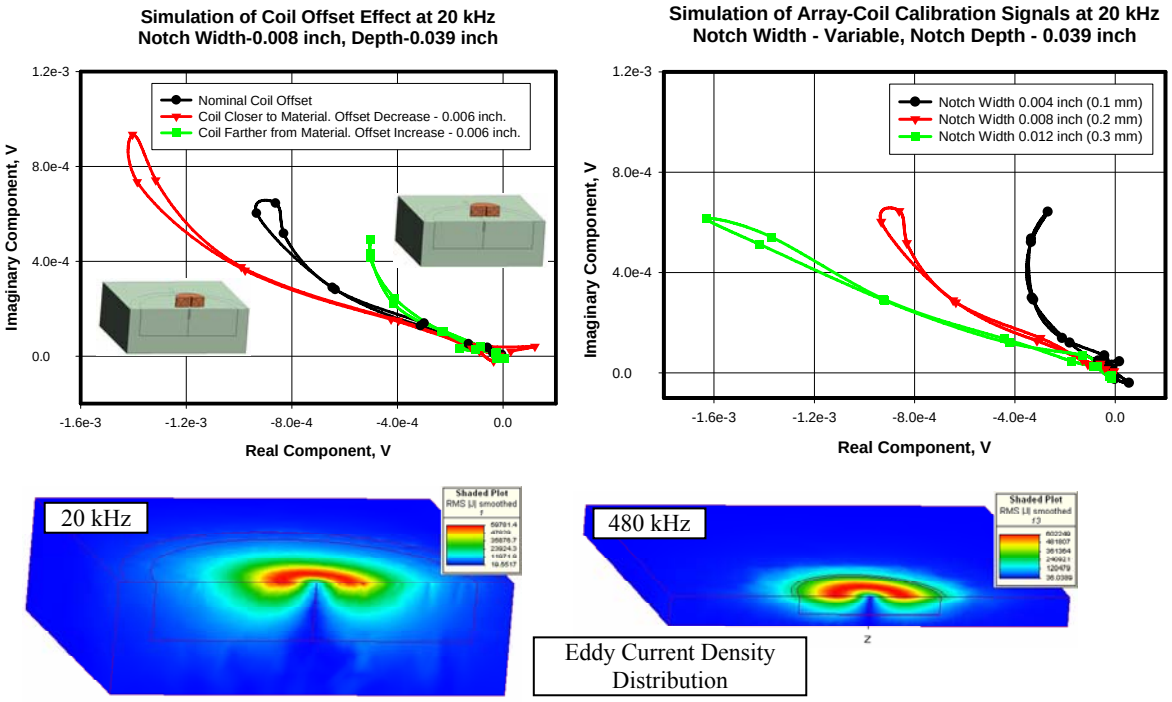

FIGURE 3. Modeling the LO and notch width effect (top) and eddy current density distribution (bottom.).

actual material. The objective function of the optimization process was set to search for minimum difference between the probe modeled and measured impedance as material properties were varied in the model. The optimization process required automated model recalculation for various combinations of σ and μ.

Once steel properties were estimated, many other variables difficult to represent through specimens was possible to model and evaluate their effect on detection and sizing such as actual depth of penetration, calibration notch width, probe field concentration with ferrites, variable probe liftoff (LO) and material properties variation. A model of a single coil from the array probe was built to simulate the inspection variable effects. Some of modeling results are illustrated in Fig. 3.

The effect of increasing and decreasing LO and calibration notch effect is shown in Fig. 3, top left. The increase or decrease of LO causes the sensitivity to decrease or increase, respectively. It means that the LO shall be maintained at minimum and any coating on the inspection surface must be accounted for during calibration. The modeling of calibration notch width effect (Fig. 3, top right) shows that the crack depth calibration will not be affected if the signal imaginary component is used for depth measurements. The LO signal (not shown) is oriented horizontally on both impedance plots.

The eddy current density distribution simulation at two frequencies is shown in Fig. 3, bottom. A comparison with standard depth of penetration estimates at lower frequency of 20 kHz indicated that the standard depth of penetration formula [1] overestimated the depth of penetration by more than two times because the coil shape effect was not accounted for.

CALIBRATION FOR DEPTH SIZING

The eddy current inspection procedures require a calibration specimen for standardizing sensitivity and sizing. A calibration specimen was manufactured from ASTM A572 Grade 50 steel (Fig. 4) to match the experimental specimen material to be tested later. The specimen allowed any probe (single or array) to be used. The specimen

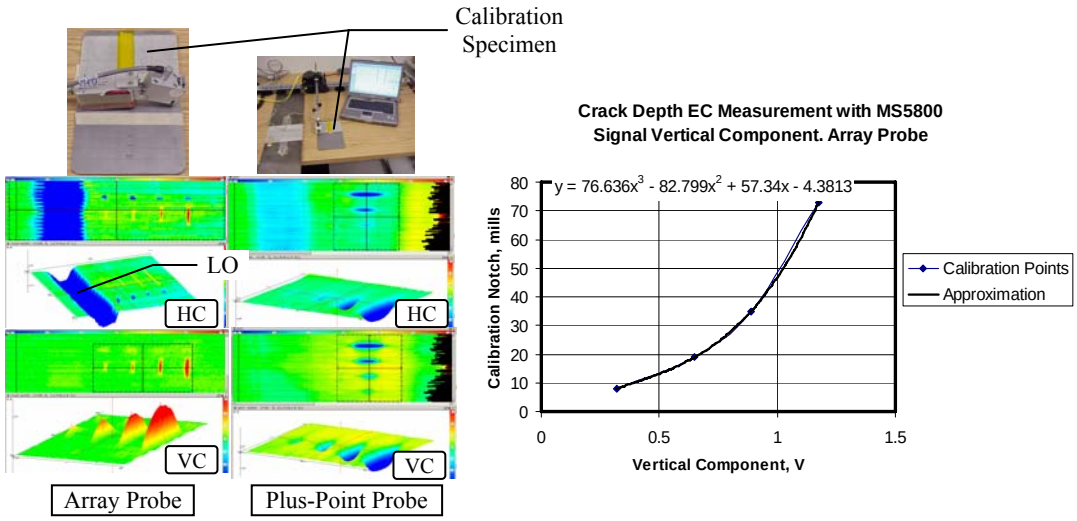

FIGURE 4. Calibration for depth sizing with array and single plus-point probe (left) and depth-sizing curve using vertical or imaginary signal component (right). (HC – horizontal signal component, VC- vertical signal component)

was 6.3-mm (0.25-in.) thick with seven shallow electrical discharge (EDM) notches – three across the entire width with various depths and three with various lengths and depths. The shorter notches have a circular shape to more closely represent fatigue crack shape. The smallest and the largest notches have length and depth 5.7 × 0.2 mm (0.22 × 0.008 in.) and 15.2 × 1.8 mm (0.6 × 0.071 in.), respectively.

Typical calibration screens with array and single plus-point probe for depth sizing are shown in Fig. 4. The calibration was performed through tape to simulate coating thickness and another tape to simulate LO. A typical depth-sizing curve using signal vertical or imaginary component is shown in Fig. 4. Other depth-sizing curves were built using signal amplitude where signal phase did not correlate with notch depth.

INSPECTION OF SPECIMENS WITH FATIGUE CRACKS

Weld surface geometry (toe-to-flat surface transition, crown curvature) and roughness present unique challenges for eddy current techniques. To adequately cover the inspection area for automated or semi-automated inspection, a special custom probe design was required that was outside of the project scope. The weld HAZ and crown of all seven specimens with fatigue cracks were raster scanned with the plus-point probe because it is specifically designed to negotiate the changes in surface roughness and geometry. The weld crown was removed on three of the specimens. Two additional probes (array and spot probe with ferrite core) were used for inspection of the three of the specimens after crown machining.

The inspection after machining was done to simulate some service conditions, to allow trials with various eddy current probes, and to assess the effect of the machining on the inspection capabilities. All eddy current inspections were conducted with a nonconductive tape covering the inspection area and simulating paint coating. The approach of using tape for coating simulation during eddy current inspection was validated through comparison with results obtained on a heavily painted specimen. The calibration and test specimens were demagnetized before inspection to eliminate the effect of possible residual magnetization on inspection results.

The AEC inspection performance was compared to two other techniques conducted on bare specimen surface. The first techniques was phased-array ultrasound testing (PA-

TABLE 1. Eddy current sizing comparison with PA UT and MP before crown machining. (D – flaw depth, L – flaw length)

NDE Method	Size (mm)	Specimen						
		W12	W13	W14	W24	W33	W41	W44
AEC	D	>2	1	>2	1.7	1.9	0.8	>2
	L	54	20.5	51	79	60	26	67
PA UT	D	5.5	1.4	4.1	3.4	4	1.1	12.7
	L	52	20	56	80	48	21	60
MP	D	-	-	-	-	-	-	-
	L	95	79	102	103	105	89	92
Fracto-graphy	D	-	-	-	5.1	-	1.4	9.1
	L	-	-	-	72.8	-	24.3	69.6

UT) for crack detection and sizing of depth and length. The other technique was MP for crack detection and length sizing only. To validate the performance of all NDE techniques, the three specimens with weld crown machined were fractured.

Depth (D) and length (L) sizing with various techniques is shown in Table 1 before machining. The length measurements with AEC were close to PA UT length measurements. MP length measurements were larger than AEC and PA UT length measurements. The fractography of the three specimens W24, W41, and W44 indicated that AEC length measurements were closest to the actual length. The MP oversized the crack length by almost 270% for Specimen W41. Comparing again the fractography and AEC depth measurements, AEC undersized the crack depth and the discrepancy increased with the increase of depth.

The fractography sections and AEC indications for the three fractured specimens are shown in Fig. 5. AEC techniques have very high resolution to small and shallow surface cracks (Specimens W41 and W24). The AEC indications are truncated for flaws deeper than 2 mm (0.079 in.) (Specimens W24 and W44). The truncated indication or depth reading close to upper limit of approximately 2 mm (see Fig. 4 and Table 1, Specimens W24 and W44) are additional clues that the cracks are deeper than the actual depth of penetration.

While crack detection and crack length measurements have been very reliable and accurate, it has been shown throughout the study that the eddy current methods will undersize the crack depth when common methodologies and procedures are used for sizing.

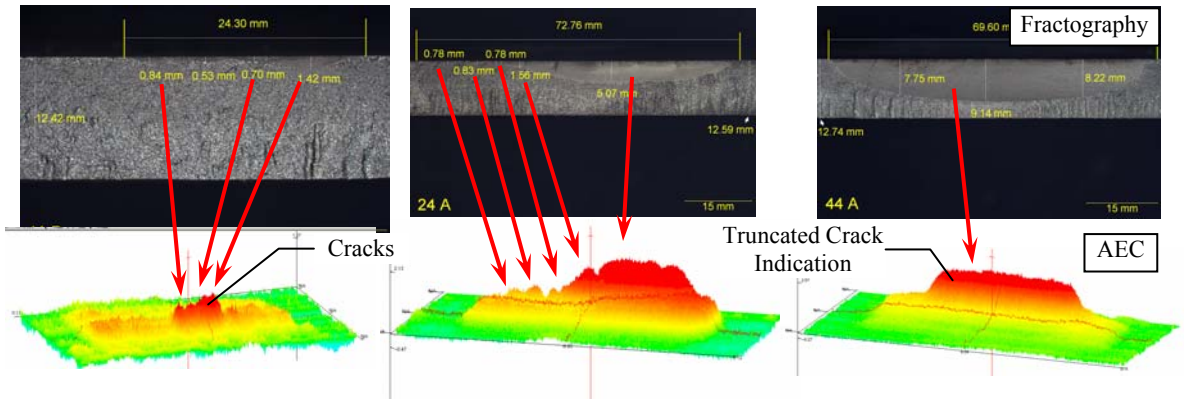

FIGURE 5. Fractography (top) and AEC (bottom) indications for the three fractured specimens W41 (left), W24 and W44 (right).

The NDE community has been cognizant about this problem for some time [2-4]. Apart from surface machining, there are two major reasons for the depth undersizing:

- The fundamental difference between the actual fatigue cracks (very tight in steel) and the EDM notches used for equipment depth sizing calibration is the first reason.
- The second reason is the difference between the geometry and roughness of the calibration specimen and the actual inspection area. The difference translates into increased LO that decreases the sensitivity and leads directly to undersizing (Fig. 3).

The ultimate solution was to produce significant number of fatigue cracks in HAZ followed by acquisition of sufficient number of eddy current measurements from the fatigue crack areas. The last stage would be destructive measurement of the actual crack depth for building depth calibration curves with the actual crack depth rather than EDM notch depth. This approach, though, was outside of the scope of the project.

Another approach reported in the literature [3] was to compare the eddy current signals from EDM notches and fatigue cracks on flat specimens, define depth correction function, and later correct the actual depth crack measurements during weld inspection. Fig. 6 demonstrates this approach for depth size correction of crack indications in W41, absolute channels at 320 kHz. It should be noted that the correction function [3] was reported for similar probe but different instrument, different steel and slightly different frequency (300 kHz) which will cause additional errors (oversizing after correction). The depth profile measurements with AEC demonstrated again the high sensitivity and resolution achievable even with off-the-shelf plus-point probes. The four peaks on AEC depth profile plot (left) are well correlated to the four cracks distinguishable on the fractography picture (right).

As mentioned above, the weld crowns of Specimens W24, W41, and W44 were machined to provide opportunity for additional trials where crown geometry would not allow adequate coverage, if present. The machining was also performed to simulated field inspections where crown removal is required by a specification (nuclear power plants). In addition, the effect of machining on flaw detectability was also investigated.

The detectability of the crack in W44 after machining was not affected (Fig. 7). The shape of the indication, though, after machining was different from the crack indication before machining. The effect of possible material smearing is visible at the middle of the crack indications. The machining did not affect PA-UT verification measurements (not shown). The crack was correctly classified as deeper than 2 mm (0.079 in.) by AEC techniques.

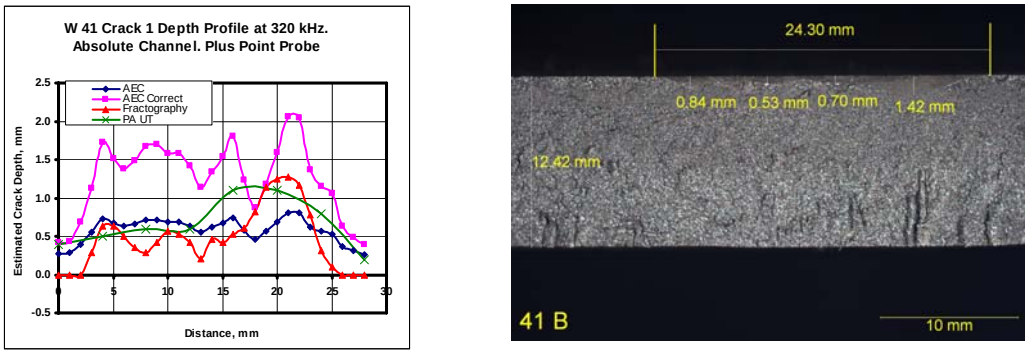

FIGURE 6. Comparison of corrected and uncorrected depth measurements for AEC to PA-UT and fractography. (Depth profile – left and fractography for W41 – right.)

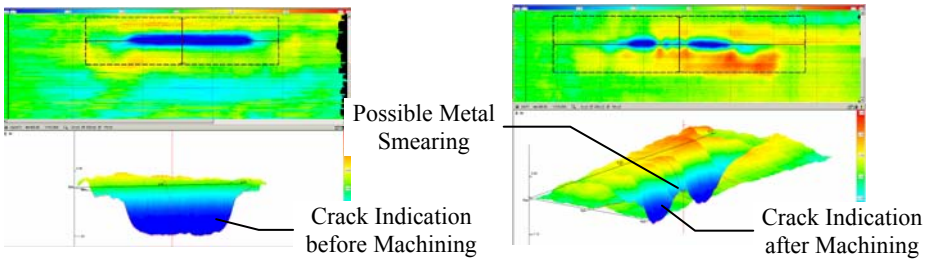

FIGURE 7. Comparison of crack indication at 20 kHz on Specimen W44 before (left) and after (right) crown machining acquired with the same probe.

As expected, the machining affected AEC and MP more than PA UT measurements. The depth sizing for AEC was affected to a greater extent than length sizing. The detectability of small flaws in Specimen W41 was reduced after machining due to the metal smearing for all three techniques AEC, PA-UT, and MP.

CONCLUSIONS

Due to the non-contact nature of eddy current techniques, AEC proved to perform reliably through thick paint coating. The following conclusions can be drawn from the work on this project:

- The AEC techniques demonstrated very good capabilities in detection and sizing of surface flaws and surface area treatments.
- The AEC were better than PA-UT and MP in detection and length sizing of small surface flaws.
- The crack depth undersizing inherent to common eddy current field procedures (confirmed in this study) can be resolved through better design of the calibration procedures.
- Machining or other smearing operations before inspection should be avoided when small crack detection and sizing is considered or additional activities should be planned to eliminate the effect of metal smearing operations.

Future studies will address the development of eddy current probes for more reliable inspection of weld structures and thicker coatings.

ACNOWLEDGMENTS

This work was performed under contract with the State of Ohio with financial support from the Ohio Department of Development. The content reflects the views of EWI and does not necessarily reflect the views of the State of Ohio, Department of Development.

REFERENCES

1. D. J. Hagemaier, *Materials Evaluation*, **43**, 1438-1442, 1454 (1985).
2. D. J. Hagemaier, M. R. Collingwood and K. H. Nguyen, *Materials Evaluation*, **50**, 1225-1231 (1992).
3. D. Lamtenzan, G. Washer and M. Lozev, "Detection and Sizing of Cracks in Structural Steel using the Eddy Current Method", U.S. Department of Transportation, Federal Highway Administration, Nondestructive Evaluation Validation Center, Report No. FNWA-RD-00-018, 22 p. (November 2000).
4. T. J. Jessop, *Metal Progress*, **123**, no. 4, 62-65 (1983).